Aust. J. Phys., 1991, **44**, 73–86

Heat Conduction through Support Pillars in Evacuated Windows

R. E. Collins, L. Poladian,[A] *B. A. Pailthorpe and R. C. McPhedran*

School of Physics, University of Sydney,
Sydney, N.S.W. 2006, Australia.
[A] Present address: Optical Sciences Centre,
Australian National University,
G.P.O. Box 4, Canberra, A.C.T. 2601, Australia.

Abstract

A study has been made of the rate of heat transport through a short pillar connecting two separated plates. Three separate approaches to the problem are discussed—analytic, numerical and experimental. The results of the different methods are in good agreement, and confirm the classical result for heat flow through a short, circular contact between semi-infinite bodies. These results are of particular relevance to the design of flat evacuated glazings incorporating short support pillars.

1. Introduction

It is possible to construct devices with extremely high levels of thermal insulation by combining the insulating properties of vacuum with the very low radiation heat transport characteristics of low emittance surfaces Such principles were first applied in the venerable dewar flask, and more recently, in evacuated tubular solar collectors (Window and Harding 1984). It has long been realised (Ortmanns 1988) that similarly high levels of thermal insulation would be very desirable in flat windows in order to minimise heat losses and gains from buildings. However, it has been generally believed that flat plate evacuated windows with useful properties were difficult, if not impossible, to produce technologically. The principal difficulties perceived were the formation of a hermetic edge seal around the periphery of the window, and the design of a method to keep the glass plates apart under the action of the very high atmospheric pressure forces, whilst retaining a high level of thermal insulation between the plates.

Recent papers (Robinson and Collins 1989; Collins and Robinson 1990) described an approach to the production of evacuated windows which offers significant promise of technological success. In this design, a low melting point glass (solder glass) is used to produce a fusion edge seal between the two glass plates. During the formation of this edge seal a small tube is also sealed into the window to permit subsequent evacuation. An array of small support pillars is disposed over the surface of the glass in order to separate the glass sheets.

0004-9506/91/010073$05.00

A principal constraint in the design of an evacuated window relates to the support pillars. These pillars must be sufficiently small in order that heat transport by thermal conduction through the pillars is below tolerable levels. Small pillars, however, result in very high levels of mechanical stress, both within the pillars themselves and within the glass in the vicinity of the pillars. The relationships between these physical effects have been derived (Robinson and Collins 1990; Collins and Robinson 1990). It has been shown that a window of satisfactory performance can be produced with an array of short pillars having a diameter of approximately 0·6 mm and a separation of about 30 mm.

The nature of the contact between two separate pieces of material has been the subject of study for over a century. In his classic paper, Hertz (1882) discussed the contact between two solids in terms of many small contacting areas. Holm (1955, 1979) used the model developed by Hertz to derive the thermal impedance of a general contact in terms of the heat flow through individual, circular contacting areas or 'spots' of negligible thickness. The thermal impedance of such spots is dependent on the material of the contacting substances and is determined by the geometry of the system. Holm (1955) derived the classical relationship for the thermal conductance of a short circular contact of radius a between two infinite materials of thermal conductivity κ:

$$C = 2\kappa a\,. \qquad (1)$$

This paper deals with the thermal conductance of window support pillars of geometry not unlike the classical contact spots discussed by Holm. In windows of interest however, it is important to consider contacts of somewhat more general geometry than those of Holm. For example, the diameter of the pillars may not be negligible compared with the thickness of the plates. In addition the height of the pillars may be significant compared with the diameter. Finally, the existence of a support pillar between two plates perturbs the temperature distribution on the inner surfaces of the plates and will therefore affect radiative heat transport between the two plates in the vicinity of the pillars.

This problem has been examined using three approaches. Firstly, an analytic method has been developed to calculate the total heat transfer by thermal conduction through a pillar, and the reduction in radiative heat transfer in the vicinity of a pillar. Secondly, finite difference calculations have been used to solve for the isotherms within the volume of the plates and the pillars. Finally, evacuated windows have been constructed and the thermal conductance of support pillars has been measured in these devices.

2. Modal Expansion Method

The geometric parameters of our model are shown in Fig. 1. We shall assume initially that the two outer surfaces of the plates are isothermal, and that the inner surfaces are adiabatic. Later, we shall include the effects of radiative transport between the two inner surfaces. A cylindrical polar coordinate system is chosen with its origin at the centre of one of the pillars.

By symmetry the plane $z = 0$ is also an isotherm. Let the temperature on this plane be T_0 and the total temperature difference across the structure be ΔT. For an infinite periodic array of pillars, the dashed lines in Fig. 1 represent planes of symmetry and therefore there is no transverse heat flux across them. Equivalently, these planes can be replaced by adiabatic boundaries. Thus the problem is reduced to a finite structure. If $d \gg a$ then the separation of the pillars will have negligible effect on the temperature profiles and heat fluxes near the pillar. Thus, for simplicity (and to retain azimuthal symmetry) we choose a circular system of radius d with a single pillar of radius a in the centre.

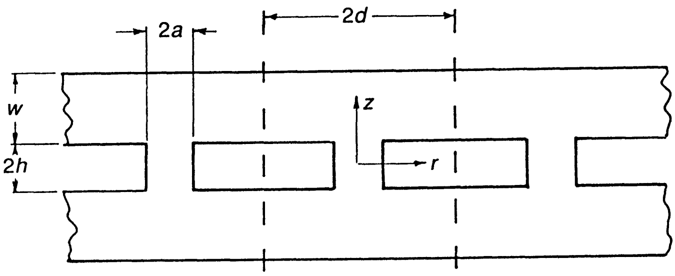

Fig. 1. Geometry of pillars and plates. The pillars are arranged in a two-dimensional periodic array and are separated by a distance $2d$. The analytic and numerical approaches consider only one pillar positioned centrally within two cylindrical plates of radius d.

We choose to work with the following normalised, non-dimensional quantities: the radial coordinate $R = r/a$, the axial coordinate $Z = z/h$, the pillar height $2H = 2h/a$, the total thickness of the plates $W = w/a$ and the pillar separation $2D = 2d/a$. The normalised temperature is given by $\tilde{T} = 2(T - T_0)/\Delta T$, where T is the temperature at any point within the system.

The appropriate boundary conditions are

$$\frac{\partial \tilde{T}}{\partial R} = 0 \qquad \text{at } R = D \qquad \text{for all } Z, \tag{2}$$

$$\frac{\partial \tilde{T}}{\partial R} = 0 \qquad \text{at } R = 1 \qquad \text{for } -H < Z < H, \tag{3}$$

$$\frac{\partial \tilde{T}}{\partial Z} = 0 \qquad \text{at } Z = \pm H \qquad \text{for } 1 < R < D, \tag{4}$$

$$\tilde{T} = \pm 1 \quad \text{at } Z = \pm(W + H) \quad \text{for all } R, \tag{5}$$

and $\tilde{T}(R, Z)$ is an antisymmetric function of Z.

The solutions to Laplace's equation in cylindrical coordinates with azimuthal symmetry are given by the products of Bessel functions of the radial coordinate and exponential (or trigonometric) functions of the axial coordinate.

The following expansion of the temperature is suitable inside the pillar

$$\tilde{T}(R,Z) = \sum_{n=0}^{\infty} A_n \frac{J_0(j_{n,1}R)}{J_0(j_{n,1})} \frac{\sinh(j_{n,1}Z)}{\sinh(j_{n,1}H)}, \tag{6}$$

for $0 < R < 1$ and $-H < Z < H$.

The $j_{n,1}$ are the zeros of the derivative of the Bessel function $J_0(z)$. This expansion automatically satisifies the boundary condition (3) and the required antisymmetry. It also simplifies at $Z = H$ and $R = 1$ to facilitate applying the boundary conditions.

The following expansion of the temperature is suitable inside the upper plate

$$\tilde{T}(R,Z) = 1 - \sum_{n=0}^{\infty} B_n J_0(j_{n,1}R/D) \frac{\sinh[j_{n,1}(W+H-Z)/D]}{\sinh[j_{n,1}W/D]}, \tag{7}$$

for $0 < R < D$ and $H < Z < H+W$. This expansion automatically satisifies the boundary conditions (2) and (5). The lower plate is treated by symmetry.

If $D \gg 1$, as is the case here, the expansion in discrete modes can be replaced by an expansion in continuous modes as is appropriate for an infinite plate:

$$\tilde{T}(R,Z) = 1 - \int_0^{\infty} \tilde{B}(x) J_0(Rx) \frac{\sinh[(W+H-Z)x]}{\sinh[Wx]} dx, \tag{8}$$

for $0 < R < \infty$ and $H < Z < H+W$.

The remaining boundary condition (4) and continuity of $\tilde{T}$ and its derivative at the boundary between the pillar and the plate are satisfied by matching the expansions and using the orthogonality properties of the Bessel functions. The following system of linear equations is obtained:

$$A_m + \sum_{n=0}^{\infty} I_{n,m}(H,W,D) A_n = \delta_{m,0}. \tag{9}$$

The matrix elements $I_{n,m}(H,W,D)$ are given by

$$I_{n,m}(H,W,D) = \sum_{l=0}^{\infty} \frac{4 j_{n,1} \coth(j_{n,1}H)}{j_{l,1} D J_0(j_{l,1})^2} \frac{(j_{l,1}/D)^2 J_1(j_{l,1}/D)^2 \tanh(j_{l,1}W/D)}{[j_{n,1}^2 - (j_{l,1}/D)^2][j_{m,1}^2 - (j_{l,1}/D)^2]}. \tag{10}$$

If $D \gg 1$ the sum can be replaced by an integral

$$I_{n,m}(H,W,D) = 2 j_{n,1} \coth(j_{n,1}H) \int_0^{\infty} \frac{x^2 J_1(x)^2 \tanh(Wx)}{[j_{n,1}^2 - x^2][j_{m,1}^2 - x^2]} dx, \tag{11}$$

with the sum and integral above being evaluated numerically.

The solution of the system of equations (9) gives the expansion coefficients A_n from which all other quantities of interest can be calculated. For example, the heat flux across the plane $z = z_0$ in the pillar is given by

$$\mathcal{F}_Q = \kappa \int_0^a \frac{\partial T(r, z_0)}{\partial z_0} 2\pi r dr$$
$$= \pi a \kappa \Delta T \int_0^1 \frac{\partial \tilde{T}(R, Z_0)}{\partial Z_0} R dR . \tag{12}$$

Using the expansion (6) and the orthogonality properties of the Bessel functions the result is

$$\mathcal{F}_Q = A_0 \kappa \frac{\pi a^2}{2h} \Delta T , \tag{13}$$

which is independent of z_0 as required by conservation of flux. Apart from the geometric factor A_0 (which depends on h, a, w and d via the matrix equation) this is the expression for the heat flux through a cylinder of length $2h$ and cross sectional area πa^2.

A similar calculation in the plates using (7) gives the result

$$\mathcal{F}_Q = B_0 \kappa \frac{\pi d^2}{2w} \Delta T . \tag{14}$$

Conservation of flux implies

$$B_0 = \frac{wa^2}{hd^2} A_0 . \tag{15}$$

There are a number of limiting cases where A_0 and hence the flux can be obtained analytically. The first case is for a pillar whose radius is much smaller than its height and also much smaller than the width of the plates and the pillar separation. Thus, $H, W, D \gg 1$ and the quantity $\coth(j_{n,1}H)\tanh(Wx)$ appearing in the matrix elements (11) becomes independent of both H and W. Since no geometric parameters appear in the equations A_0 must be a constant. Thus for $a \ll h, w, d$ the flux is proportional to the square of the radius and inversely proportional to the height of the pillar. For such a structure, the entire temperature drop occurs across the pillar and there is very little effect from the presence of the plates. The result obtained is in fact that for plane laminar flow through a cylinder of length $2h$ and radius a and thus $A_0 = 1$ and

$$\mathcal{F}_Q = \kappa \frac{\pi a^2}{2h} \Delta T . \tag{16}$$

The next case is for a pillar whose radius is much larger than its height and also much larger than the thickness of the plates. Thus, $H, W \ll 1$ but $D \gg 1$ and the quantity $j_{n,1} \coth(j_{n,1}H)\tanh(Wx)$ becomes $(w/h)x$. Thus A_0 is independent of a and is a function only of w/h. In particular if $w \gg h$ the diagonal terms in the matrix are negligible and A_0 is linearly proportional to h/w. Thus for $d \gg a \gg w \gg h$ the flux is proportional to the square of the radius and inversely proportional to the width of the structure. The result obtained is in fact that for plane laminar flow through a cylinder of length $2w$ and radius a, and thus $A_0 = h/w$ and

$$\mathcal{F}_Q = \kappa \frac{\pi a^2}{2w} \Delta T. \tag{17}$$

The final (and most relevant) case is for a pillar whose radius is much larger than its height but whose radius is much smaller than the width of the plates and the pillar separation. Thus, $H \ll 1$ and $W,D \gg 1$ and the quantity $j_{n,1} \coth(j_{n,1}H) \tanh(Wx)$ becomes $(a/h)x$. Thus A_0 is independent of w and is a function only of a/h. In particular if $a \gg h$ the diagonal terms in the matrix are negligible and A_0 is linearly proportional to h/a. Numerically the coefficient of proportionality is indicated to be $4/\pi$. Thus for $w,d \gg a \gg h$ the flux is directly proportional to the radius and independent of the height of the pillar:

$$\mathcal{F}_Q = 2\kappa a \Delta T. \tag{18}$$

This is the classical result derived by Holm (1955).

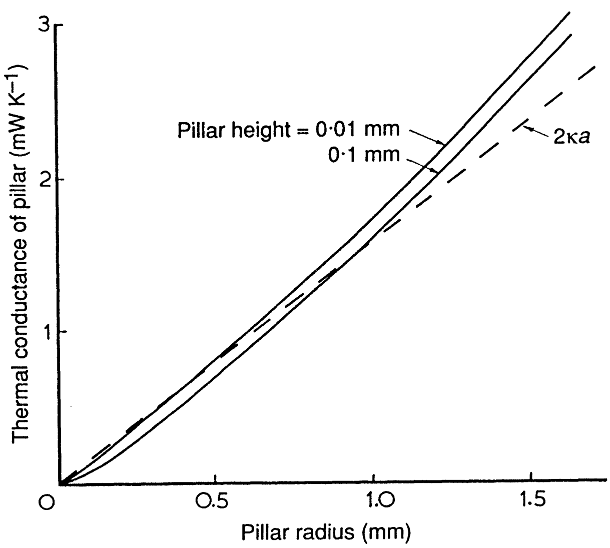

Fig. 2. Thermal conductance of a single pillar between two sheets of 4 mm thick glass, as a function of pillar radius. Results are shown for two different heights of the pillar, and the classical result for negligible height is also drawn for comparison.

Typical results for the effective thermal conductance ($\mathcal{F}_Q/\Delta T$) of individual pillars of height 0·01 and 0·1 mm are shown in Fig. 2, for glass of thickness 4 mm. Also shown for comparison is the $2\kappa a$ result for a pillar of zero thickness.

Heat Transferred by Radiation

The heat transferred per unit area by radiation between two infinite plane parallel surfaces at temperatures T_1 and T_2 with emissivity ϵ is given by

$$\frac{\epsilon\sigma}{2-\epsilon}(T_1^4 - T_2^4) \approx \frac{4\epsilon\sigma T_{av}^3}{2-\epsilon}\Delta T, \tag{19}$$

where σ is the Stefan–Boltzmann constant. The second form is suitable if $\Delta T \ll T_{av}$ where T_{av} is the average of T_1 and T_2.

We calculate radiative heat transfer through the vacuum gap on the assumption that this effect is sufficiently small that it does not significantly alter the temperature distribution within the plates. This will be seen to be a good approximation. We also assume that the rate of radiative heat transfer at any point is proportional to the local temperature difference across the gap at that point. For windows with a very small gap, this is certainly a good approximation. The heat transferred by radiation between the inner surfaces of the system is thus given by

$$\begin{aligned}\mathcal{R}_Q &= \frac{4\epsilon\sigma T_0^3}{2-\epsilon}\int_a^d [T(r,h) - T(r,-h)]2\pi r dr \\ &= \frac{4\epsilon\sigma T_0^3}{2-\epsilon}2\pi a^2\Delta T\left[\int_0^D \tilde{T}(R,H)RdR - \int_0^1 \tilde{T}(R,H)RdR\right].\end{aligned} \tag{20}$$

The first integral is evaluated using the expansion (7) and the second integral is evaluated using the expansion (6). Using the orthogonality properties of the Bessel functions the result is

$$\begin{aligned}\mathcal{R}_Q &= \frac{4\epsilon\sigma T_0^3}{2-\epsilon}2\pi a^2\Delta T[(1-B_0)D^2 - A_0] \\ &= \frac{8\epsilon\sigma T_0^3}{2-\epsilon}\left(\pi d^2 - \frac{w+h}{h}\pi a^2 A_0\right)\Delta T,\end{aligned} \tag{21}$$

where the second expression is obtained using (15).

The two terms appearing above have the following physical interpretation. The first term is the total heat that would be radiated through an area πd^2 in the absence of the pillar. The other term represents a decrease in the amount of radiated heat because of the presence of the pillar. A simplistic argument would suggest that this amount is given by the area of the pillar πa^2 or more possibly by the quantity $\pi a^2 A_0$ (see equation 13). In fact, it is greater than this amount because the presence of the pillar reduces the temperature difference between the inner surfaces near the pillar and hence the heat radiated between these surfaces. The decrease in the radiated heat is related to the flux through the pillar by

$$\mathcal{D}_Q = \frac{8\epsilon\sigma T_0^3}{2-\epsilon}\pi a^2\,\frac{w+h}{h}A_0\Delta T = \frac{8\epsilon\sigma T_0^3}{2-\epsilon}\,\frac{w+h}{\kappa}\mathcal{F}_Q. \tag{22}$$

Thus the total increase in heat flux due to the presence of a single pillar (as compared with a system with no pillars) is

$$\mathcal{F}_Q - \mathcal{D}_Q = \left(1 - \frac{8\epsilon\sigma T_0^3}{2-\epsilon}\,\frac{w+h}{\kappa}\right)\mathcal{F}_Q . \tag{23}$$

For a typical evacuated window structure, $w = 4$ mm, $h \ll w$ and $\kappa = 0 \cdot 78\ \mathrm{W\,m^{-1}\,K^{-1}}$ for soda lime glass. For uncoated glass ($\epsilon = 0 \cdot 84$), the measured heat flux through a pillar will thus be about $4 \cdot 7\%$ less than that expected from purely geometric considerations. For windows incorporating low emittance coatings ($\epsilon \sim 0 \cdot 1$), the correction for the radiation decrease is negligible.

Our procedure of first calculating the temperature profile in the absence of radiation with adiabatic boundaries, and then calculating the radiated heat from the profiles obtained is valid provided $\mathcal{D}_Q \ll \mathcal{F}_Q$. This is the case for all geometries of interest in the window application.

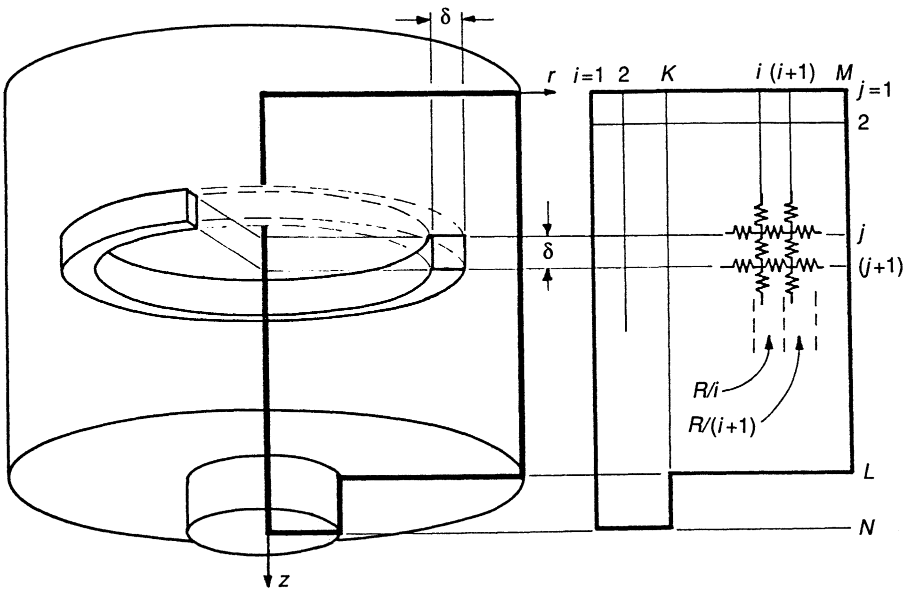

Fig. 3. Definition of the resistive network for the numerical analysis.

3. Temperature Profile—Finite Difference Calculation

A straightforward method of calculating the temperature profile in the system studied (Fig. 1) is provided by a resistive network model (Fig. 3). Focussing on a single pillar and assuming cylindrical symmetry, the resistive elements in the plates are thin concentric rings of volume $2\pi r dr dz$ (Fig. 3). In this part of the analysis, we take $z = 0$ at the outer surface of one of the plates. At fixed radius r the vertical resistance of the element is

$$R_z = \frac{dr}{2\pi\kappa r dz}, \tag{24}$$

where κ is the thermal conductivity of the plate. The corresponding radial resistance of the element is

$$R_r = \frac{dz}{2\pi\kappa r dr}. \tag{25}$$

It is clear that modelling the plate as a square lattice of thermal resistors means that the resistance values increase at larger radii but are independent of height at any given radius. Temperatures are sampled on a lattice of points [$r = (i-1)\delta$, $z = (j-1)\delta$; cf. Fig. 3] and heat flows along thermal resistive elements connecting lattice points when temperature differences exist. The reduced temperature $\tilde{T}(r,z)$, where $\tilde{T} = 1$ on the outer glass surface and $\tilde{T} = 0$ in the vacuum, is represented by the array

$$T_{ij} = \tilde{T}((i-1)\delta, (j-1)\delta). \tag{26}$$

Since thermal energy does not accumulate at any point within the system, an equation balancing heat flows can be written for each lattice point. In the plates, away from edges and corners, the recurrence relation is formed by balancing four heat flows:

$$[(T_{i+1,j} - T_{i,j}) + (T_{i,j+1} - T_{ij}) + (T_{i,j-1} - T_{ij})](i) + (T_{i-1,j} - T_{ij})(i-1) = 0. \tag{27}$$

Near corners, edges and interfaces only two or three heat flows are balanced, and the relevant recursion relations are easily derived. For example, at $i = M$, no radial heat flow occurs. The bottom edge of the glass sheet ($j = L$), adjacent to the vacuum space, will have small radiative heat losses. For small temperature differences the radiative heat losses can be linearised as discussed above (equation 19), and represented by conduction through an equivalent resistor:

$$\dot{Q} \approx \frac{4\sigma\epsilon T^3}{2-\epsilon}\Delta T \equiv \frac{\Delta T}{R_{vac}}$$

and $R_{vac} = CR_{plate}$. The recurrence relation at the bottom edge of the plate for $K < i < M$ is

$$[(T_{i,L-1} - T_{i,L}) + (T_{i+1,L} - T_{i,L})]i + (T_{i-1,L} - T_{i,L})(i+1) + (T_{i+1,L+1} - T_{i,L})\frac{i}{C} = 0. \tag{28}$$

In systems of interest, such as for glass evacuated windows, this radiative heat transfer is considerably smaller than conduction heat transfers within the plates and will be neglected here ($C \to \infty$). Thus heat flows only along the bottom edge of the plate. An analogous relation holds at the outer edge of the glass pillar ($i = K$ for $M < j < N$). The axis of symmetry ($r = 0, i = 1$) has no radial heat flow so that the appropriate recurrence relation is

$$T_{1,j-1} + T_{2,j} + T_{1,j+1} - 3T_{1,j} = 0. \tag{29}$$

Finally, the boundary conditions are

$$T_{i,1} = 1 \tag{30}$$

and

$$T_{i,N} = 0, \qquad i < K \tag{31}$$

at outer and inner surfaces, respectively.

Equations (27)–(29) can be solved by iteration for a chosen geometry, subject to the boundary conditions (30) and (31). The initial conditions for interior lattice points can be taken as either $T = 0$ or as a linear temperature profile. Lattice spacings of $0 \cdot 1$ mm for the plates and $h/10$ for the vertical direction in the pillar are found to be adequate. Of order 1000–2000 iterations are required.

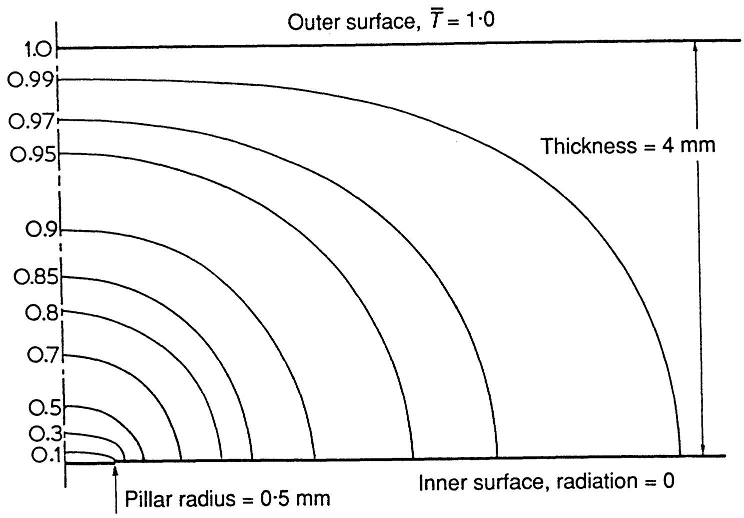

Fig. 4. Isotherms for heat flow through a single cylindrical pillar between two flat glass plates. Radiative heat flow through the vacuum gap is assumed to be zero.

A typical temperature profile for glass of thickness 4 mm and pillars of height $0 \cdot 01$ mm and radius of $0 \cdot 5$ mm is shown in Fig. 4.

These data may be used to calculate the temperature gradient at a plane in the solid which upon integration gives values for the total heat flow through the pillar. It is found that the values of heat transport obtained in this way agree with those determined by the analysis of the previous section to within ±10%. This is about the expected accuracy of the numerical method given the size of the radial grid in the vicinity of the pillars (10 elements). Higher accuracy could be obtained with finer grids and is indeed observed with larger pillars, but little further useful information is obtained with this refinement.

4. Experimental Methods

Evacuated windows have been constructed using the method shown in Fig. 5 and described in more detail elsewhere (Collins and Robinson 1990). A

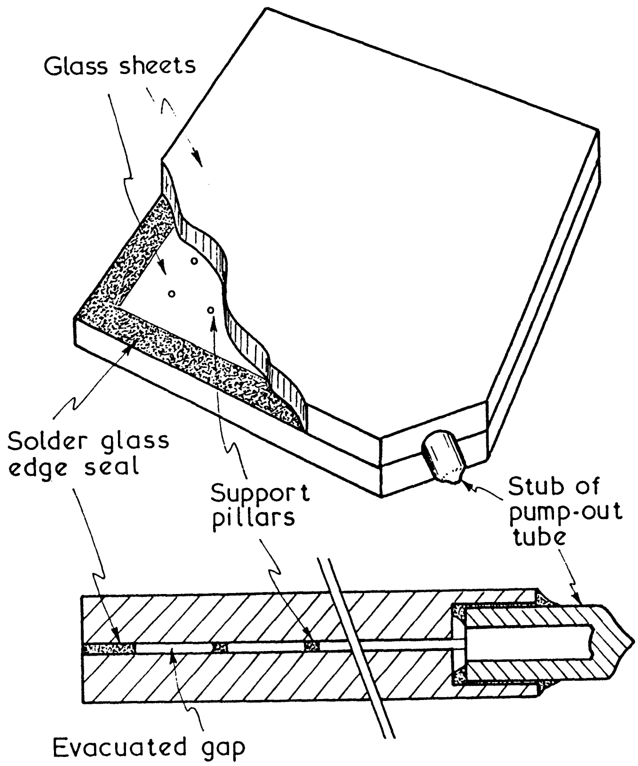

Fig. 5. Schematic diagram (not to scale) illustrating the construction of an all-glass evacuated window.

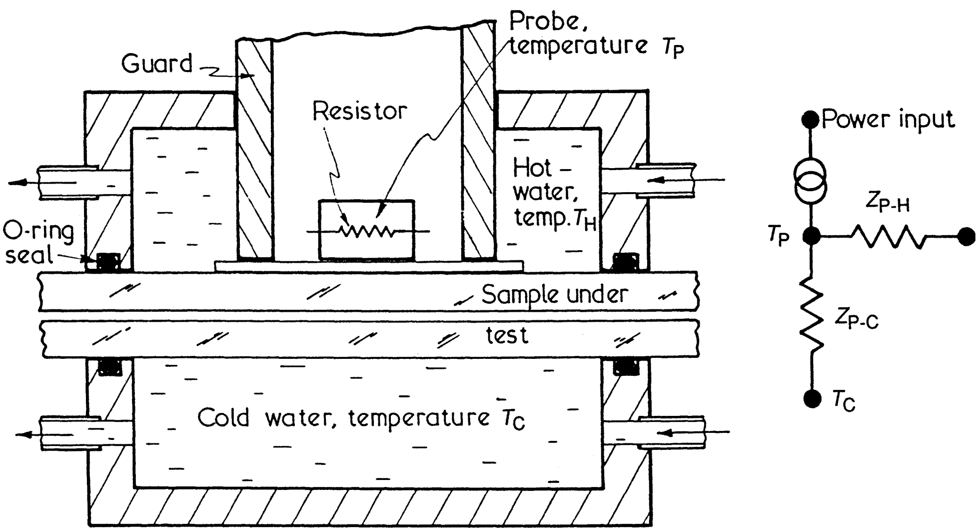

Fig. 6. Diagram of the apparatus for measuring heat flow through an evacuated window. Also shown is the thermal equivalent circuit for the system.

hermetic seal is made between the edges of two sheets of glass using low melting point glass (solder glass). This material is also used to fuse a small diameter pump-out tube into a cavity which has been previously machined in the mating surfaces of the glass sheets. The solder glass is used to make small diameter, short cylindrical pillars which form a square array over the surface of the glass sheets.

Of principal interest in this paper is the heat transport through the support pillars. Such heat transport is measured using an apparatus illustrated schematically in Fig. 6. A small cylinder, called the probe, is located within a thermal guard which is held at constant temperature by circulating water. The probe and guard are joined to a glass sheet, 1 mm thick, which is pressed against one side of the window to be measured. The other side of the window is held at a constant lower temperature, again by circulating water. The temperatures of the probe, the guard, and the cold water are measured by thermocouples. Power can be supplied to the probe by a thermal resistor embedded within it. The thermocouple, and power leads from the probe, are thermally terminated on the guard before emerging from the apparatus.

The equivalent thermal circuit of the measuring instrument is also shown in Fig. 6. In this electrical analogy, temperatures become voltages, thermal impedances become electrical impedances, and heat flow is replaced by current. The temperature of the probe is determined by the relative thermal impedances between the probe and the guard Z_{P-H}, and the probe and the cold water Z_{P-C}. If the latter impedance is extremely high, the temperature of the probe will be very close to that of the guard. A measurement of probe temperature as a function of power into the probe gives a straight line, confirming the simple thermal impedance model described above.

The situation when the probe and guard temperatures are equal is of particular interest. Under these conditions, all heat flow from the probe is through the window. This heat flow can therefore be used to calculate the thermal conductance of the window given a knowledge of the area of the probe. In the small area measuring device constructed, the probe is 10 mm diameter and the inside diameter of the guard is 20 mm. The effective surface area of the probe is therefore not known very accurately. A calibration is performed by measuring an evacuated window assembly which is pumped dynamically. In such a device it is known that the internal pressure is so low that gas conduction is negligible. The effective diameter of the probe, determined using published values for emittance of glass (0·84), turns out to be 14·0 mm, for the windows studied here which consist of two glass sheets, each 4 mm thick.

Measurements were first made of the heat transport through the vacuum space of the window, and then of heat flow through a pillar and the vacuum space surrounding that pillar. The heat flow through the pillar can be obtained from the difference of these two quantities. A more accurate estimate includes the correction for the reduction in radiative heat transfer in the area surrounding the pillar due to the perturbation of the temperature of the inner surfaces of the glass plates by the pillar. For surfaces of emittance 0·84 this correction amounts to some 4·7% as calculated by the analytic approach discussed above.

Fig. 7 shows the experimental results for thermal conductance of pillar structures as determined by this method. Also shown for comparison is the classical Hertzian result for very short pillars. The pillars measured are approximately 0·01 mm high as determined by counting interference fringes within the evacuated gap. The diameters of the pillars are measured directly through the surface of the glass plates.

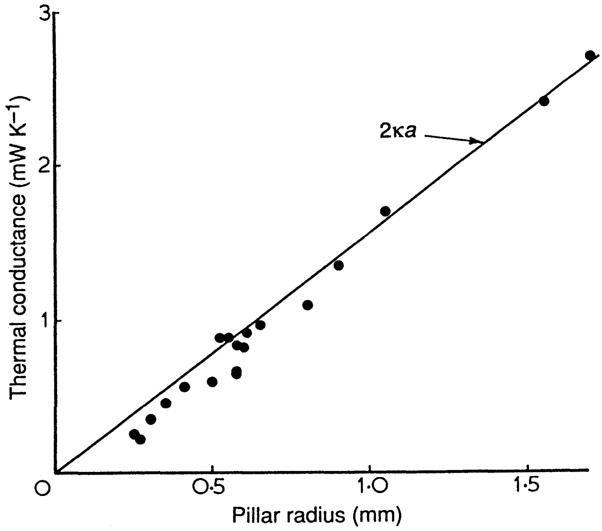

Fig. 7. Data for thermal conductance for individual contact pillars in an all-glass evacuated window. A correction of 4·7% has been added to the experimental measurements to account for the local reduction of radiative heat flow in the vicinity of the pillars. The classical result for pillars of negligible height is also shown.

5. Discussion

The initial motivation for undertaking this work was aimed at the practical understanding of an important heat transfer process in evacuated windows. Whilst the classical result of Holm (1955) for heat transport at short contacts was well established, the geometry of the support pillars in evacuated windows can be more complex. In addition the modification of radiative heat transport in the vicinity of the pillars required elucidation. The results for heat flow through the pillars obtained by the three different approaches are consistent. The analytic and numerical approaches yield similar values for total heat transport through a pillar, and these data are in good agreement with the experimental results over the relevant range of sizes. The classical result is also confirmed.

The results from the two calculational methods for radiation depression in the vicinity of the pillars warrant some discussion. The analytic approach predicts a value for reduction in radiative heat transport based on a perturbation method. The temperature at the inner surface of the plate is determined on the assumption of zero radiation and the radiative heat transport is calculated from this temperature difference. This approach assumes that the presence of radiative heat transport does not significantly alter the temperature distribution within the plate. This is certainly the case close to the pillar. At large distances from the pillar, however, this approximation breaks down. This can be seen from the plot of isotherms within the plates (Fig. 4). These data are also calculated for zero radiation. In a window made up of two sheets of uncoated ($\epsilon = 0 \cdot 84$) glass, 4 mm thick, it turns out that approximately 5% of the temperature difference between the outer surface and the midplane appears across the glass, and 95% across the vacuum, for regions remote from the pillar. Thus the $0 \cdot 95$ isotherm should become tangential to the inner surface at large distances from the pillar. This turns out to be significant in the estimation of radiation decrease as determined by numerical evaluation of the data of Fig. 4. Whilst the temperature depression at the inner surface decreases rapidly away from the pillar, the contribution to radiation depression at any radius is weighted by a $2\pi r$ factor. The relevant integral in equation (20) converges slowly. The precise value of radiation depression depends on many factors including thickness, thermal conductivity, and emittance of the window material. The figure of $4 \cdot 7$% derived for uncoated, 4 mm thick glass is obviously an upper estimate. For low emittance glass, equation (23) would give a more accurate estimate. In all cases, however, the radiation depression is either small or negligible.

In summary, the three methods discussed here give consistent results for the rate of heat transport through support pillars in an evacuated window. The results are also in agreement with the classical value for pillars of negligible height. The methods complement each other in that they provide different types of data on this system. The alternative perspectives resulting from the various approaches provide enhanced insights into the nature of the heat transfer process.

Acknowledgments

This work was supported in part by His Royal Highness Prince Nawaf bin Abdul Aziz of the Kingdom of Saudi Arabia through the Science Foundation for Physics within the University of Sydney.

References

Collins, R.E., and Robinson, S.J. (1990). *Solar Energy*, to be published.
Hertz, H. (1882). *J. Reine Angew. Math.* **92**, 156.
Holm, R. (1955). 'Electrical Contacts Handbook', 3rd edn (Springer-Verlag: Berlin).
Holm, R. (1979). 'Electrical Contacts, Theory and Application', 4th edn (Springer-Verlag: Berlin).
Ortmanns, G. (1988). Proc. ISES Solar World Congress, Hamburg (Pergamon: Oxford).
Robinson, S.J., and Collins, R.E. (1989). Proc. ISES Solar World Congress, Kobe, Japan (Pergamon: Oxford).
Window, B., and Harding, G.L. (1984). *Solar Energy* **32**, 609.

Manuscript received 20 June, accepted 17 July 1990